

Multiple Scattering of X-rays by Amorphous Samples*

BY B. E. WARREN & R. L. MOZZI

Research Laboratory of Electronics, Massachusetts Institute of Technology, Cambridge, Massachusetts, U.S.A.

(Received 14 February 1966)

An exact expression in the form of a double integral is obtained for the ratio of the intensity of double scattering to that of single scattering $I(2)/I(1)$ for a diffractometer sample of an amorphous material. By expressing the double scattering in terms of the independent scattering of the atoms, and approximating this quantity by an expression involving two parameters, the double integral is evaluated and tabulated as a function of 2θ and the two parameters. With these tabulated values, the ratio $I(2)/I(1)$ for unmodified scattering only, or for both unmodified and modified scattering, can be obtained for a sample of any composition. For the unmodified scattering from vitreous SiO_2 using Rh $K\alpha$ radiation, the value of $I(2)/I(1)$ is about 0.08 in the range $2\theta = 90^\circ$ to $2\theta = 180^\circ$. In general the second order scattering is large enough to require a correction.

In the scattering of X-rays by amorphous samples, the main contribution to the intensity arriving at the point of observation is due to single scattering of the primary beam by each volume element dV_1 . There is also a contribution at the point of observation due to the scattered intensity from dV_1 being scattered again by another volume element dV_2 in the sample. In addition to this double scattering process, there can, of course, be a series of higher order scattering processes. We shall consider here only the double scattering process since it represents the major part of the multiple scattering.

We consider a flat faced diffractometer sample whose horizontal surface is represented by OO' in Fig. 1. The power in the primary beam is given by $P_0 = I_0 A_0$, where A_0 is the cross-sectional area. The primary beam and the direction of measurement each make an angle θ with the sample surface. It is convenient to introduce the term 'unit of composition', where for example in vitreous silica the obvious unit of composition would be one silicon and two oxygen atoms. Let n be the number of units of composition per unit volume, and let $J(2\theta_1)$ be the first order intensity in electron units per unit of composition for scattering at an angle $2\theta_1$. We first neglect the effect of absorption and the polarization factor.

* This work was supported principally by the Joint Services Electronics Program [Contract DA 36-039-AMC-03200(E)].

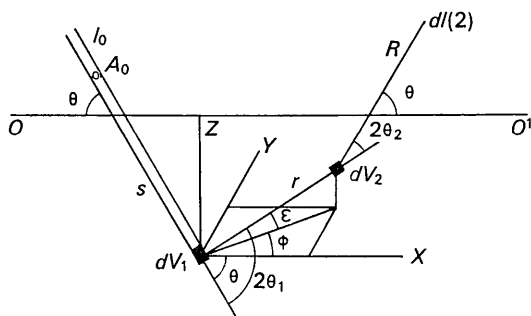


Fig. 1. Geometry of the double scattering process in a diffractometer sample of an amorphous material.

Let dI_r be the intensity at distance r from the volume element dV_1 due to scattering of the primary beam by dV_1 .

$$dI_r = I_0 \frac{e^4}{m^2 c^4 r^2} J(2\theta_1) n A_0 ds.$$

Let $dI(2)$ be the intensity at the point of observation at distance R from the sample, due to the scattering of the intensity dI_r by the volume element dV_2 .

$$dI(2) = dI_r \frac{e^4}{m^2 c^4 R^2} J(2\theta_2) n dV_2.$$

In terms of a small solid angle $d\Omega$ centered on the line r , we express the second volume element by $dV_2 = r^2 d\Omega dr$, where $d\Omega = \cos \epsilon d\epsilon d\varphi$. Combining the previous equations we obtain

$$dI(2) = P_0 \left(\frac{e^4}{m^2 c^4} \right)^2 \frac{n^2}{R^2} J(2\theta_1) J(2\theta_2) \cos \epsilon d\epsilon d\varphi ds dr. \quad (1)$$

The angle ϵ which is shown in Fig. 1 is the angle which the direction r makes above the horizontal plane XY . For positive values of ϵ , the path length in the sample is $2s + r(1 - \sin \epsilon / \sin \theta)$. In the integrations arising from equation (1), r goes from $r = 0$ to $r = s \sin \theta / \sin \epsilon$, and assuming a thick sample, s goes from zero to infinity. Allowing now for absorption, the two integrals are readily evaluated.

$$\int_{s=0}^{\infty} \int_{r=0}^{s \sin \theta / \sin \epsilon} \exp[-\mu\{2s + r(1 - \sin \epsilon / \sin \theta)\}] dr ds = \frac{\sin \theta}{2\mu^2(\sin \theta + \sin \epsilon)}. \quad (2)$$

For negative values of ϵ , the integrations for both r and s are from zero to infinity. The result is again given by equation (2), if we replace $\sin \epsilon$ by its magnitude $|\sin \epsilon|$.

If an unpolarized beam is scattered first through an angle $2\theta_1$, and the scattered beam then scattered through an angle $2\theta_2$, so that the final direction makes an angle 2θ with the original primary beam, the polarization factor is expressed by

$$(PF) = [\cos^2 2\theta_1 + \cos^2 2\theta_2 + (\cos 2\theta_1 \cos 2\theta_2 - \cos 2\theta)^2] / 2. \quad (3)$$

Introduce the abbreviations $p_1 = \cos 2\theta_1$ and $p_2 = \cos 2\theta_2$. From the spherical triangles involved in Fig. 1,

$$p_1 = \cos 2\theta_1 = \cos \theta \cos \varphi \cos \varepsilon - \sin \theta \sin \varepsilon, \\ p_2 = \cos 2\theta_2 = \cos \theta \cos \varphi \cos \varepsilon + \sin \theta \sin \varepsilon. \quad (4)$$

Since the intensities of first order scattering can equally well be represented as functions of p_1 and p_2 , we shall now replace $J(2\theta_1)$ and $J(2\theta_2)$ by $J(p_1)$ and $J(p_2)$. Combining equations (1) and (2), and adding the polarization factor, the intensity $I(2)$ is given by

$$I(2) = P_0 \left(\frac{e^4}{m^2 c^4} \right)^2 \frac{n^2}{R^2} \frac{\sin \theta}{2\mu^2} \int_{\varphi=-\pi}^{\pi} \int_{\varepsilon=-\pi/2}^{\pi/2} J(p_1) J(p_2) (PF) \cos \varepsilon d\varepsilon d\varphi \\ \times \frac{\sin \theta + |\sin \varepsilon|}{\sin \theta + |\sin \varepsilon|}. \quad (5)$$

In changing from a value ε to a value $-\varepsilon$, there is no change in the integrand of equation (5) except that p_1 and p_2 are interchanged. Hence we can limit the integration with respect to $d\varepsilon$ to the range $\varepsilon=0$ to $\varepsilon=\pi/2$ and multiply the expression by 2. There is no change in the integrand of equation (5) on replacing φ by $-\varphi$, and we can again multiply by 2 and restrict the integration to the range $\varphi=0$ to $\varphi=\pi$. In changing from an angle φ to the angle $\pi-\varphi$, $\cos \varphi$ is replaced by $-\cos \varphi$. From equation (4), it follows that p_1 changes to $-p_2$ and p_2 changes to $-p_1$. There is no change in the polarization factor (PF), and hence by adding $J(-p_1)J(-p_2)$ in the integrand, the integration over φ can be reduced to the range $\varphi=0$ to $\varphi=\pi/2$.

$$I(2) = P_0 \left(\frac{e^4}{m^2 c^4} \right)^2 \frac{n^2}{R^2} \frac{2 \sin \theta}{\mu^2} \int_0^{\pi/2} \int_0^{\pi/2} [J(p_1)J(p_2) + J(-p_1)J(-p_2)] (PF) \cos \varepsilon d\varepsilon d\varphi. \quad (6)$$

The ratio n/μ is conveniently expressed by $n/\mu = N / \sum_i A_i \mu_i(m)$ where N is the Avogadro number, the sum is over the unit of composition, and A_i and $\mu_i(m)$ are the atomic weights and mass absorption coefficients of the atoms.

For an unpolarized primary beam, the corresponding first order intensity $I(1)$ is given by

$$I(1) = P_0 \left(\frac{e^4}{m^2 c^4} \right) \frac{1}{R^2} \left(\frac{1 + \cos^2 2\theta}{2} \right) J(2\theta) \frac{n}{2\mu}. \quad (7)$$

Dividing equation (6) by equation (7), we obtain the ratio

$$\frac{I(2)}{I(1)} = \left(\frac{e^4}{m^2 c^4} \right) \frac{8N \sin \theta}{(1 + \cos^2 2\theta) J(2\theta) \sum_i A_i \mu_i(m)} \\ \times \int_0^{\pi/2} \int_0^{\pi/2} \frac{[J(p_1)J(p_2) + J(-p_1)J(-p_2)]}{\sin \theta + \sin \varepsilon} \\ \times (PF) \cos \varepsilon d\varepsilon d\varphi. \quad (8)$$

Since the integrations in equation (8) result in an averaging of $J(p_1)J(p_2)$ over a range of angles, it is a good enough approximation for amorphous samples to replace $J(p)$ by the independent scattering. In doing this, we use either $\sum_i f_i^2$ or $\sum_i [f^2 + i(M)]_i$ depending on

whether the measurements are to include only the unmodified intensity or both the unmodified and modified components.

It is convenient to have approximate numerical values from equation (8) without needing to carry out the integrations for each sample. For this purpose we can use the approximate representation

$$J(p) = B \left(q + \frac{1-q}{1+b \sin^2 \theta} \right) \quad (9)$$

where $B = \sum_i Z_i^2$. With this representation, the integrations in (8) have been carried out for a series of values of 2θ , q , and b to give the values of the function $Q(2\theta, q, b)$ which are recorded in Table 1. By means of the function $Q(2\theta, q, b)$, the intensity ratio is expressed in the simple form

$$\frac{I(2)}{I(1)} = \frac{B^2 Q(2\theta, q, b)}{J(2\theta) \sum_i A_i \mu_i(m)}. \quad (10)$$

To use equation (10), we plot the independent scattering curve $J(p)$ against $\sin \theta$, using either $\sum_i f_i^2$ or $\sum_i [f^2 + i(M)]_i$ depending on whether the experiment includes only the unmodified scattering or both the

Table 1. Values of $Q(2\theta, q, b) \times 10^4$

2θ	$q=0.00$					
	$b=10$	$b=20$	$b=40$	$b=60$	$b=80$	$b=100$
30	192	104	50.8	31.3	21.6	16.0
60	196	87	33.7	18.3	11.7	8.1
90	164	64	22.2	11.5	7.1	4.8
120	124	45	14.9	7.6	4.6	3.2
150	103	36	11.9	6.0	3.7	2.5
180	98	34	11.1	5.6	3.4	2.3
	$q=0.05$					
30	219	126	68.1	46.2	34.9	28.1
60	238	121	59.1	39.4	30.1	24.7
90	218	105	51.9	35.7	28.1	23.7
120	179	86	43.9	31.1	25.0	21.4
150	156	75	39.4	28.3	23.0	19.8
180	150	73	38.1	27.5	22.4	19.4
	$q=0.10$					
30	250	154	92	68	55	47
60	287	163	93	70	58	51
90	279	155	92	71	61	54
120	241	136	83	66	57	51
150	216	123	77	61	53	48
180	209	120	75	60	52	47
	$q=0.20$					
30	326	225	157	130	115	106
60	402	268	188	159	144	134
90	423	283	204	175	160	151
120	386	263	193	168	154	146
150	355	244	182	158	146	138
180	347	239	178	156	143	136

unmodified and modified components. An approximate fit to this curve is then obtained by a proper choice of the parameters q and b in equation (9). When only unmodified scattering is being considered, the best fit is usually obtained with $q=0.0$, but when the interest is in both the unmodified and modified intensities, it is necessary to use a value of q other than zero. An exact fit is of course not to be expected, but if the departures are small and equally positive and negative, the errors are largely cancelled by the averaging which is involved. Suitable values of q and b having been determined, the values of $Q(2\theta, q, b)$ are obtained by interpolation from Table 1. With the use of equation (10), the ratio $I(2)/I(1)$ can be plotted over the desired range of 2θ .

As an illustration of the magnitude of second order scattering, we can take the example of vitreous SiO_2

with Rh $K\alpha$ radiation and an experimental technique which measures only the unmodified intensity (Warren & Mavel, 1965). From equation (8) we obtain for $I(2)/I(1)$ a value of about 0.08 in the range $2\theta=90^\circ$ to $2\theta=180^\circ$. Except for samples with high absorption coefficients, the second order scattering is in general large enough to require a correction.

This work was done in part at the Computation Center at the Massachusetts Institute of Technology, Cambridge. One of us (RLM) is a Raytheon Graduate Program Member at M.I.T.

References

- WARREN, B. E. & MAVEL, G. (1965). *Rev. Sci. Instrum.* **36**, 196.

Acta Cryst. (1966). **21**, 461

Diffraction Contrast in Electron Microscopy of Chrysotile

BY E. J. W. WHITTAKER*

Ferodo Limited, Chapel-en-le-Frith, Stockport, England

(Received 24 February 1966)

Previous theoretical work on diffraction by chrysotile has not revealed the particular regions of the fibrils from which particular diffraction maxima originate. Difficulties in localizing these regions are overcome by a Fourier-transform method, and the results are applied to evaluating electron screening functions across the width of such fibrils on the basis of simple kinematical theory. The results show that under appropriate conditions electron micrographs of chrysotile fibrils may be expected to simulate hollow tubes even though the centres of the fibrils are filled either with amorphous material or with oriented ribbons of serpentine material.

Introduction

Electron microscopy provided the first evidence that chrysotile has a tubular structure (Turkevitch & Hillier, 1949; Bates, Sand & Mink, 1950). The evidence for this conclusion was based on the fact that electron microscope images of single chrysotile fibres frequently showed a central light band running along the length of the fibre with a darker band at each side. The

* Present address: Department of Geology & Mineralogy, Oxford, England.



Fig. 1. The variation in material thickness across a section of a thick-walled hollow cylinder.

boundaries between the light and dark bands are often remarkably sharp. This appearance has always been attributed to shielding of the electron beam by the fibre, this shielding being assumed to be a function of the material thickness traversed by the beam. Fig. 1, showing the variations in thickness across the section of a hollow cylinder, was used to demonstrate the theory by Noll & Kircher (1951). These workers extended the observations to stereoscopic electron micrographs of synthetic chrysotile, which gave a particularly convincing appearance of hollowness. Subsequent analysis of X-ray diffraction patterns of chrysotile showed these to be explicable in terms of cylindrically curved layers with a radius of the same order as that of the tubes deduced from electron microscopy, the layers being stacked together in numbers corresponding to the apparent wall-thicknesses of such tubes (Whittaker, 1953, 1956, 1957; Jagodzinski & Kunze, 1954; Jagodzinski, 1961). It has also been shown (Whittaker,